Reducing Reaction of Fe_3O_4 in Nanoscopic Reactors of a-CNTs

Fangyu Cao,[†] Kaifu Zhong,[†] Aimei Gao,[‡] Changle Chen,[§] Quanxin Li,[‡] and Qianwang Chen*,[†]

Hefei National Laboratory for Physical Sciences at Microscale and Department of Materials Science & Engineering, University of Science & Technology of China, Hefei 230026, P. R. China

Received: September 18, 2006; In Final Form: December 14, 2006

A reduction of Fe_3O_4 nanowires in nanoscopic reactors of amorphous C:H nanotubes (a-CNTs) was taken to understand features of the chemical reaction mechanism in nanoscale reactors. Fe_3O_4 nanowires encapsulated in a-CNTs were reduced into iron at a relatively low temperature of 570 °C, producing iron nanoparticles encapsulated in CNTs accompanied by the crystallization of the a-CNT shell. It was found that carbon in the a-CNT shell rather than hydrogen (5.5 wt % in it) reduced Fe_3O_4, showing features different from those in a macroscopic system. The possible mechanisms behind this phenomenon are discussed.

Introduction

Nanoscopic reactions have gained wide interest because of their mechanism and high activity different from macroscopic reactions. A carbon nanotube (CNT), like a nanometer-sized test tube, could be used as a nanoscopic reactor with motion restricted to a quasi-one-dimensional environment.[1] Several successful applications have been reported, including synthesis of nanostructured materials in the cavity of CNTs under mild conditions (e.g., SiC,[2−4] β-zeolite,[5] $CoFe_2O_4$,[5] GaN,[6] SiC−SiO*x* biaxial nanowires,[7] Si−B−C−N nanocables,[8] and heterostructures of CNTs and carbide nanorods[9]), focusing on making different kinds of nanometer-sized heterostructures by filling the cavity of CNTs with heterogenities or by decorating the outside surfaces of them. Some chemical reactions confined within these nanometer-sized channels exhibited higher activities.[4,5,10] However, chemical reactions that take place in the filled CNTs or heterostructures of them with other materials have rarely been reported. As an example, Bao et.al.[11] found that α-Fe_2O_3 nanoparticles in the cavity of CNTs were reduced by them at 600 °C, and those adhered at the outside wall were reduced at 800 °C, while α-Fe_2O_3 powder was reduced by graphite when the temperature was higher than 1000 °C, implying that the reactions exhibited higher activities.

Recently, we developed a one-pot method for the synthesis of Fe_3O_4/amorphous C:H nanotube (a-CNT) coaxial nanocables by pyrolysis of ferrocene in Sc−CO_2 at 400 °C.[12] In the as-prepared products, single-crystal Fe_3O_4 nanowires with a diameter of around 40 nm are continuously covered by a-CNT shell. The a-CNT shell is rich in hydrogen (elemental analysis shows that H% in the a-CNTs' shell is as high as 5.5 wt %.), which releases in the form of molecular H_2 from 400 °C. This cable-like nanostructure provides a natural nanometer-sized a-CNT test tube filled with Fe_3O_4 nanowires. a-CNTs with a hollow cavity can also be obtained from the Fe_3O_4/a-CNT nanocables by acid disposal. In this work, we present experimental evidence of facile reduction of Fe_3O_4 nanowires located in the cavities of a-CNTs to Fe nanoparticles at around 570 °C, vs reduction of powdered Fe_3O_4 by a-CNTs mechanically mixed together at higher temperature (>700 °C), as an example of chemical reactions of obtaining CNT-confined metallic nanoparticles through direct reduction of incorporated oxide nanowires in nanometer-sized reactors.

Experimental Section

Heat treatment of the Fe_3O_4/a-CNT nanocables was taken in quartz boat heating by a tube furnace in N_2 stream, with a flow rate of 100 mL/min. The rate of heat increase of the system was 10 °C/min, and the temperature was held for 10 min when it came to certain temperature points. Gas effluents were collected and injected into a Finnigan Trace 2000-MS Gas Chromatography/Mass Spectrometer for analysis, and the solid products were saved for further characterizations. In control experiments, a-CNTs and a mixture of 0.06 g of a-CNTs and 0.04 g of commercial Fe_3O_4 (CP) powder were also treated with high temperature by a tube furnace in N_2 stream, respectively. Heat treatment of a-CNTs was taken in temperature-programmed desorption (TPD) with heating rate of 10 °C/min. In the heating process, gas effluents such as H_2 ($m/e = 2$), H_2O ($m/e = 18$), and CO_2 ($m/e = 44$) were continuously monitored by a Blazers GSD300 Omnistar quadrupole mass spectrometer. The powder X-ray diffraction (XRD) analyses were performed on a Rigaku D/MAX-γA X-ray diffractometer equipped with Cu Kα radiation ($\lambda = 1.542$ Å) over the 2θ range of 10−70×bc. Transmission electron microscopy (TEM) analyses were performed on a Hitachi H-800 transmission electron microscope with electron diffraction, and the accelerating potential is 200 kV. High-resolution TEM (HRTEM) images were taken on a JEOL-2010 with an accelerating voltage of 200 kV. Magnetic measurements were carried out on a Riken BHV-55 vibrating sample magnetrometer (VSM).

Results and Discussion

Heat treatment of the Fe_3O_4/a-CNT nanocables at various temperatures was performed under high-purity N_2 stream. From XRD patterns of the solid products (Figure 1), it can be found that the main solid components changed from Fe_3O_4 and a-CNTs

* To whom correspondence should be addressed. E-mail: cqw@ustc.edu.cn. Fax: (+86)551-3631760.

[†] Hefei National Laboratory for Physical Sciences at Microscale and Department of Materials Science & Engineering, University of Science & Technology of China.

[‡] Department of Chemical Physics, Lab of Biomass Clean Energy, University of Science & Technology of China.

[§] Department of Chemistry, The University of Chicago, 5735 South Ellis Avenue, Chicago, Illinois.

10.1021/jp0661037 CCC: $37.00
Published on Web 02/01/2007

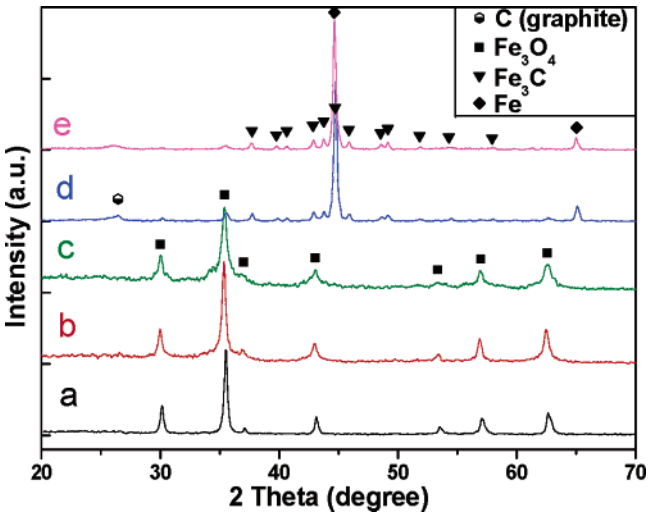

Figure 1. XRD patterns of the Fe_3O_4/a-CNT nanocables heated to (a) 409 °C, (b) 468 °C, (c) 533 °C, (d) 570 °C, and (e) 595 °C and then cooled down in an N_2 stream. Peaks of the compounds were labeled on the patterns.

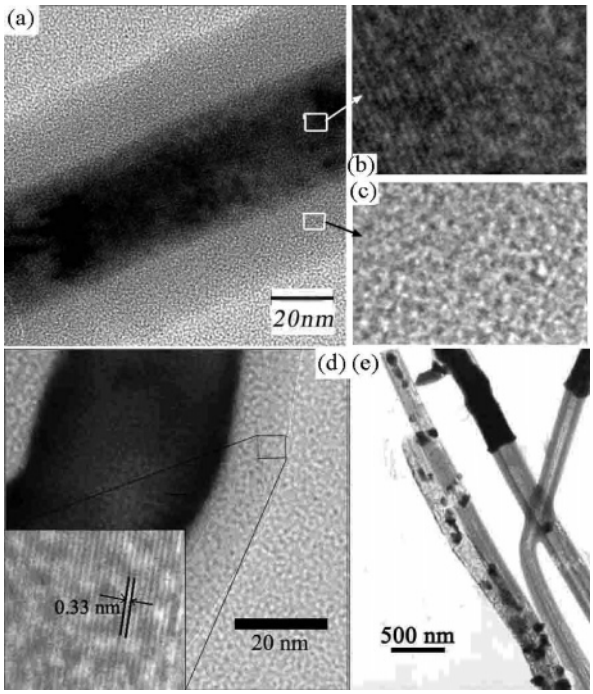

Figure 2. HRTEM images of the Fe_3O_4/a-CNT nanocables (a)[12] before and (d) after annealing at 570 °C. Parts (b) and (c) are partial enlarged images of (a), and (e) is a TEM panorama of (d).

to iron and graphitic CNTs, with some Fe_3C as byproducts. Reduction of Fe_3O_4 to Fe happened at a temperature (called Tc) between 532 and 570 °C, much lower than the temperature needed to reduce pulverous Fe_3O_4 by graphite (>1100 °C); carbonization of the a-CNT shells happened at the same temperature, also much lower than the reported temperature (>1700 °C),[13] indicating a simultaneous quick reduction of Fe_3O_4 nanowires and crystallization of a-CNTs. The HRTEM image (Figure 2d) shows that the whole a-CNT shell has changed from amorphous carbon to graphitic CNTs at 570 °C, with a *d* value of 0.33 nm, very close to that of graphite (002).

Heat treatment of a-CNTs and a mixture of commercial Fe_3O_4/a-CNTs were both taken as control experiments. In Figure 3a, each of the XRD patterns exhibit a broad peak, typical of a-CNTs. With the temperature elevated, the peaks become

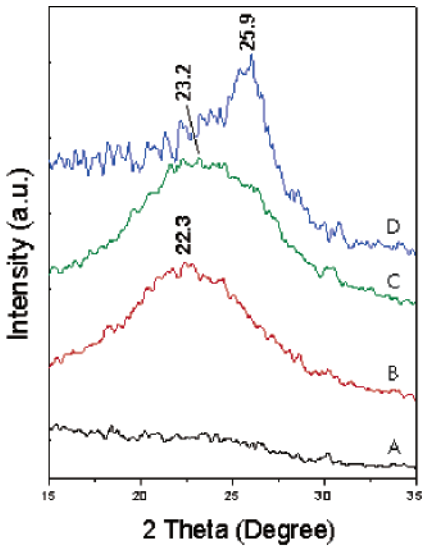

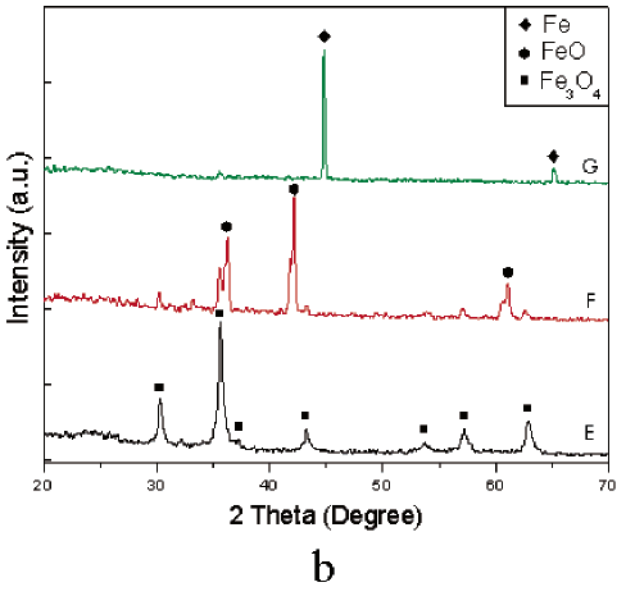

Figure 3. XRD patterns of (a) the a-CNTs heated to (A) 400 °C, (B) 600 °C, (C) 700 °C, and (D) 800 °C and (b) the mixture of commercial Fe_3O_4 powders and a-CNTs heated to (E) 700 °C, (F) 800 °C, and (G) 900 °C and then cooled down in N_2 stream. Peaks of the compounds were labeled on the patterns.

sharper and shaper, and the center of them moves toward 26.6°, which is the position of the graphite (002) crystal plane, showing better crystallization of the a-CNTs by heating under higher temperature. The crystallization temperature of the hollow a-CNTs is much higher than that of a-CNTs in Fe_3O_4/a-CNT nanocables, implying that encapsulated Fe_3O_4 nanowires may contribute to the crystallization, producing Fe/Fe_3C catalysts. Figure 3b shows that the Fe_3O_4 powders in the mixture were not reduced until heated to 800 °C, indicating that reduction of the unencapsulated Fe_3O_4 is harder than encapsulated ones. The σ-electron density in CNTs shifting from the concave inner to the convex outer surface caused by the deviation from planarity may contribute to the temperature difference.[14,15] The interaction between the electron-deficient concave surface of the nanotube and the anionic oxygen in encapsulated Fe_3O_4 nanowires could lead to weakened bonding strength of Fe_3O_4 and hence lower the activation energy for the reduction in the cavity.[11] Thus, Fe could form at a very low temperature of Tc. In contrast, for the

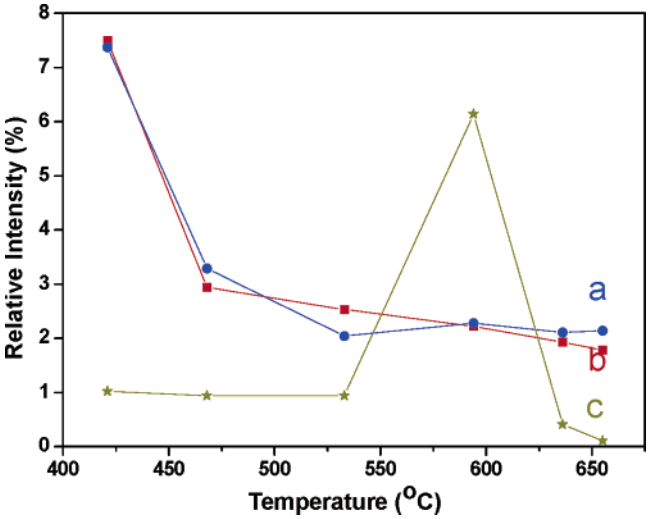

Figure 4. Ratios of (a) O_2, (b) H_2O, and (c) CO_2 fractions in gas effluents of heat treatment of the Fe_3O_4/a-CNT nanocables at different temperatures.

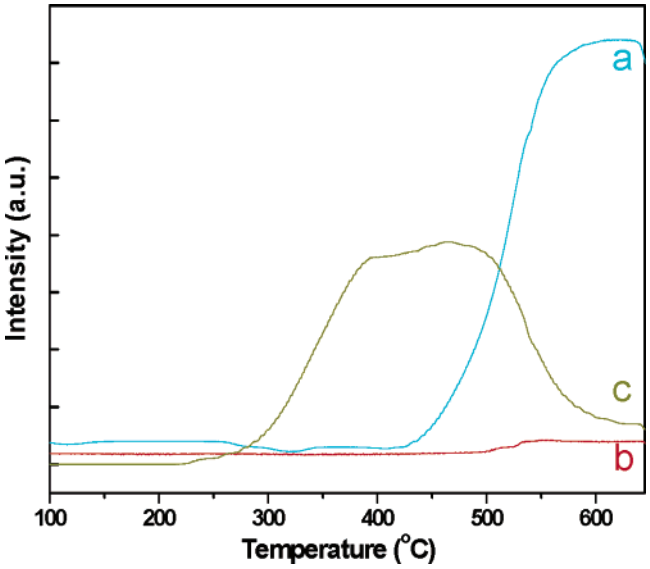

Figure 5. (a) H_2, (b) H_2O, and (c) CO_2 TPD of a-CNTs.

outer particles, the interaction of the electron-density-enriched outer nanotube surface with the oxygen in Fe_3O_4 should be weakened,[11] and a higher temperature to reduce Fe_3O_4 is needed, as observed. Defects in a-CNTs may also contribute to the facile reduction of Fe_3O_4 nanowires, lowering the reaction temperature.

Both the reduction of unencapsulated Fe_3O_4 powder and the crystallization of a-CNTs are imperfect at 800 °C, which is higher than Tc. It is inferred that the activation energy of reduction of Fe_3O_4 nanowires and crystallization of a-CNTs in the Fe_3O_4/a-CNT nanocables are lowered in the Fe_3O_4/a-C cable-like system, so that the two happen together at a low temperature. There are various reports regarding Fe catalyzing the crystallization of graphite and/or CNTs in the processes of synthesizing or annealing, first forming Fe_3C as an intermediate product and then obtaining CNTs from decomposing them.[16−19] In our experiment, the final solid products of annealing the nanocables are graphitic CNTs, Fe, and a little Fe_3C.

To understand the mechanism of the reaction, gas effluents released at the selected temperature points in the heating process of the Fe_3O_4/a-CNT nanocables were analyzed with mass spectrometry. By setting the intensity of the N_2 fractions peak ($m/e \sim 28$) in the gas mixture as 100%, the intensities of the peaks of different fractions are shown in Figure 4. CO_2 fractions ($m/e \sim 44$) started to be released before 400 °C, reached their maximum at around 594 °C, close to Tc, and then decreased soon. H_2 fractions ($m/e \sim 2$) cannot be detected because of their lower molecular weight than He carrier used in the instrument. O_2 fractions ($m/e \sim 32$) that were detected came from air leaked into the collection, whose amount was almost invariable. The other composites, such as H_2O fractions ($m/e \sim 18$), fluctuated inconspicuously by temperature, implying that they were not main products of the reaction but came from other routes such as desorption of planar water or decomposition of a-CNT.

For comparison, the TPD of the a-CNTs was carried out in vacuum and the slowly released gas effluents were monitored by an online quadrupole mass spectrometer (TPD-MS, Figure 5). CO_2, formerly presented as adsorbed CO_2 or carbonyl, ether, and/or other surface oxygen groups in the carbon shell,[20] was released between 300 and 600 °C. The peaking temperature of the releasing rate of CO_2 is about 460 °C, far from that of heating Fe_3O_4/a-CNT nanocables, indicating that the released CO_2 in the latter experiment should be the product of the reaction of encapsulated Fe_3O_4 nanowires with an a-CNT shell, different from that released from heating pure a-CNTs. H_2 became the obvious gas product after 400 °C, accompanied by a little water vapor possibly produced by the reaction between H_2 and released CO_2 or air leaked into the instrument.

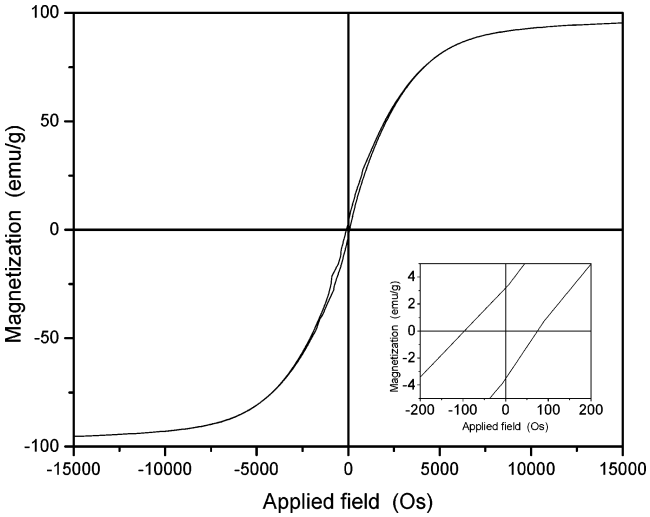

Figure 6. M−H hysteresis loops for the samples after annealing, measured at room temperature. The insert shows detail of the remnant magnetization and coercive field.

The M−H hysteresis loop (Figure 6) measured at room temperature shows that the powder sample after annealing exhibits ferromagnetism, with a saturation magnetization, Ms = 93 emu/g; remnant magnetization, Mr = 3 emu/g; and coercive field, Hc = 85 Oe. The Ms value is much lower than 220 emu/g of the corresponding bulk iron,[21] which could be due to the considerable mass of carbon and the nanoscopic size of the iron particles. Correspondingly, the data of the sample before annealing is Ms = 27.5 emu/g, Mr = 12.7 emu/g, and Hc = 324.5 Oe.[12] In addition, iron nanoparticles with oxide impurity are known to exhibit Hc values larger than 1000 Oe,[22] while the Hc values of our products are relatively low. This implies that a thorough transformation from iron oxide to iron was happening during the annealing process.

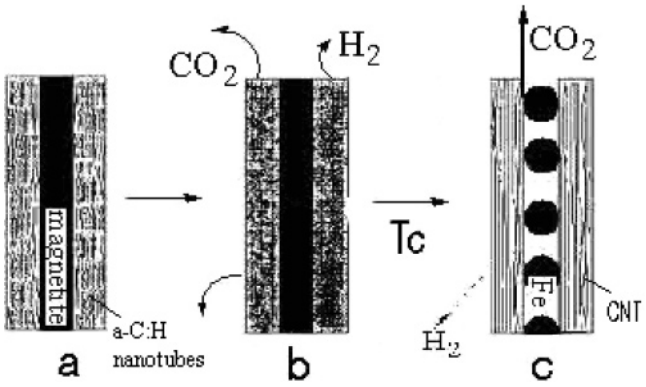

Figure 7. Mechanism of the nanoscopic reaction: a → b shows the process of releasing gas effluents form a-CNTs at low temperature; b → c shows the process of reducing Fe_3O_4 by carbon accompanied with the graphitization of a-CNTs; 532 °C < Tc < 570 °C.

According to the experimental results, one clearly sees that it is carbon rather than H_2 released from a-CNTs reduced Fe_3O_4 nanowires, with itself oxidized to CO_2

$$Fe_3O_4 + \text{a-CNTs} \xrightarrow{Tc} Fe + C(\text{graphitic}) + H_2 + CO_2$$

A model (as shown in Figure 7) of the reduction of Fe_3O_4 coupled with the crystallization of a-CNT is proposed. As shown in the HRTEM images (Figure 2), the a-CNTs consist of small graphene sheets. First, the graphene sheets start to decompose at a temperature lower than Tc, releasing gas products such as CO_2, H_2, water vapor, and so forth, and leaving a-CNTs full of defects and unsaturated carbon atoms. When the temperature rises to Tc, the a-CNTs reduce Fe_3O_4 to Fe metal, releasing CO_2 as a byproduct. CO is also a possible product of the reaction.[11] However, because the molecular weight ($M_w \sim 28$) of CO is the same as N_2, the carrier gas used in the system, the existence of CO cannot be verified by the mass spectrometric method. Catalyzed by the as-produced Fe metal nanoparticles, the graphene sheets change to small graphitic crystallites, with Fe_3C as an intermediate product. Due to the catalyzation of the metallic Fe, the crystallization of a-CNT proceeds faster. As a result, once the reaction starts, it goes along fast and comes to an end soon, within several minutes. To reduce the surface energy, the iron atoms start bonding together. At last, metallic Fe nanoparticles grow and small graphitic crystallites reorient and merge to form a three-dimensional graphitic nanotube order, as a process expected to bring about by itself a negative free energy change.[13] These Fe particles are separated instead of continuous in CNTs, different from the encapsulated Fe_3O_4 nanowires, because the volume of iron is not enough to fill the cavity of a-CNTs. If only a few iron nucleating points form at the beginning of the growth process, the Fe atoms may accumulate on them and form particles of large sizes, while many nucleating points dispersing in one nanocable may lead to small dispersed particles.

Though it was possible that released H_2 might reduce Fe_3O_4 at even lower temperature (e.g., 260 °C) based on thermodynamic data,[23] no obvious quantitative change of H_2O in gas effluents was found, showing that H_2 was not the reductant in our experiment. A possible reason is that hydrogen cannot easily enter into a nanotube reactor to take part in reactions. It is reported that a-C:H coatings may decrease the permeation properties of H_2, N_2, O_2, and CO_2.[24] As mentioned above, Fe_3O_4 nanowires were encapsulated in a-CNTs. At high temperature, the released H_2 tend to diffuse to the exterior rather than the cavity of the a-CNT shell, which lies over the Fe_3O_4 nanowires and prevents H_2 from diffusing through it. The released H_2 was soon expelled from the experimental system by an N_2 stream. Experimentally, H_2 was detected to be released from a-CNTs between 300 and 600 °C, as shown in Figure 5. As a result, the concentration of H_2 in the system remained at a low level out of the a-CNT shell, and there was almost no H_2 in the cavity of it. Therefore, it was hardly possible for H_2 to meet Fe_3O_4 nanowires by diffusing through the a-CNT shell. In contrast, there is no barrier between a-CNTs and Fe_3O_4 nanowires in the nanometer-sized reactor, which makes the reaction more kinetically favored. Thus, the Fe_3O_4 nanowires were reduced by carbon rather than hydrogen in the reaction. Further research is needed to better understand the reaction.

Conclusions

A facile reducing reaction of Fe_3O_4 nanowires in the Fe_3O_4/a-CNT nanocables to metallic Fe nanoparticles by the a-CNTs at Tc (532 °C < Tc < 570 °C) was observed. Though H_2 started to release at a low temperature of 400 °C, it did not take the role of reductant to reduce Fe_3O_4 nanowires because it tends to diffuse to the exterior of the nanotubes and then escape form the reaction system rather than to diffuse to the interior part of them. In contrast, carbon in a-CNTs functioned as a reductant, reducing Fe_3O_4 to metallic Fe, and carbon itself was oxidized to CO_2. Graphitization of a-CNTs occurred simultaneously with the reducing reaction at relatively low temperature of Tc. The studies reveal that a gas such as hydrogen cannot easily enter into a nanotube reactor to take part in reactions, which could provide information for reactions occurring in a confined system and help to develop nanoscopic reactors and synthesize new nanostructured materials.

Acknowledgment. This work was supported by the Natural Science Foundation of China (20125103 and 90206034).

Supporting Information Available: Synthesis, magnetic properties, XRD, TEM, FESEM, FTIR, and elemental analysis of the sample before annealing and details of GC-MS data are available. This material is available free of charge via the Internet at http://pubs.acs.org.

References and Notes

(1) Dujardin, E.; Ebbesen, T. W.; Hiura, H.; Tanigaki, K. *Science* **1994**, *265*, 1850.
(2) Dai, H. J.; Wong, E. W.; Lu, Y. Z.; Fan, S. S.; Lieber, C. M. *Nature* **1995**, *375*, 769.
(3) Pan, Z.; Lai, H. L.; Au, F. C. K.; Duan, X. F.; Zhou, W. Y.; Shi, W. S.; Wong, N.; Lee, C. S.; Wong, N. B.; Lee, S. T. *Adv. Mater.* **2000**, *12*, 1186.
(4) Sun, X. H.; Li, C. P.; Wong, W. K.; Wong, N. B.; Lee, C. S.; Lee, S. T.; Teo, B. K. *J. Am. Chem. Soc.* **2002**, *124*, 14464.
(5) Nhut, J. M.; Pesant, L.; Tessonnier, J. P.; Winé, G.; Guille, J.; Pham-Huu, C.; Ledoux, M. J. *Appl. Catal. A.* **2003**, *254*, 345.
(6) Han, W. Q.; Fan, S. S.; Li, Q. Q.; Hu, Y. D. *Science* **1997**, *277*, 1287.
(7) Wang, Z. L.; Dai, Z. R.; Gao, R. P.; Bai, Z. G.; Gole, J. L. *Appl. Phys. Lett.* **2000**, *77*, 3349.
(8) Zhang, Y.; Suenaga, K.; Colliex, C.; Iijima, S. *Science* **1998**, *281*, 973.
(9) Zhang, Y.; Ichihashi, T.; Landree, E.; Nihey, F.; Iijima, S. *Science* **1999**, *285*, 1719.
(10) Zhang, Y.; Zhang, H. B.; Lin, G. D.; Chen, P.; Yuan, Y. Z.; Tsai, K. R. *Appl. Catal., A* **1999**, *187*, 213.
(11) Chen, W.; Pan, X. L.; Willinger, M.-G.; Su, D. S.; Bao, X. H. *J. Am. Chem. Soc.* **2006**, *128*, 3136.
(12) Cao, F. Y.; Chen, C. L.; Wang, Q.; Chen, Q. W. *Carbon* **2007**, doi: 10.1016/j.carbon.2006.11.030.
(13) Ci, L. J.; Wei, B. Q.; Xu, C. L.; Liang, J.; Wu, D. H.; Xie, S. S.; Zhou, W. Y.; Li, Y. B.; Liu, Z. Q.; Tang, D. S. *J. Cryst. Growth* **2001**, *233*, 823.

(14) Haddon, R. C. *Science* **1993**, *261*, 1545.
(15) Ugarte, D.; Chatelain, A.; de Heer, W. A. *Science* **1996**, *274*, 1897.
(16) Oya, A.; Otani, S. *Carbon* **1981**, *19*, 391.
(17) Hernadi, K.; Fonseca, A.; Nagy, J. B.; Bernaerts, D.; Lucas, A. A. *Carbon* **1996**, *34*, 1249.
(18) Müller, T. E.; Reid, D. G.; Hsu, W. K.; Hare, J. P.; Kroto, H. W.; Walton, D. R. M. *Carbon* **1997**, *35*, 951.
(19) Cantoro, M.; Hofmann, S.; Pisana, S.; Scardaci, V.; Parvez, A.; Ducati, C.; Ferrari, A. C.; Blackburn, A. M.; Wang, K. Y.; Robertson, J. *Nano Lett.* **2006**, *6*, 1107.
(20) Boehm, H. P. *Carbon* **2002**, *40*, 145.
(21) Klabunde, K. J.; Zhang, D.; Glavee, G. N.; Sorensen, C. M.; Hadjipanayis, G. C. *Chem. Mater.* **1994**, *6*, 784.
(22) Gangopadhyay, S.; Hadjipanayis, G. C.; Dalc, B.; Sorensen, C. M.; Klaubunde, K. J.; Papaefyhymjou, V.; Kostikas, A. *Phys. Rev. B* **1992**, *45*, 9778.
(23) Tiernan, M. J.; Barnes, P. A.; Parkes, G. M. B. *J. Phys. Chem. B* **2001**, *105*, 220.
(24) Vasquez-Boruchi, S.; Jacob, W.; Achete, C. A. *Diamond Relat. Mater.* **2000**, *9*, 1971.